J. Fluid Mech. (2006), *vol.* 569, *pp.* 259–286.
doi:10.1017/S0022112006002801 Printed in the United Kingdom

Hierarchical structures in a turbulent free shear flow

By XIAO-QIN JIANG[1,2], HAO GONG[1], JIAN-KUN LIU[1,4], MING-DE ZHOU[1,3] AND ZHEN-SU SHE[1,4]†

[1]State Key Laboratory for Turbulence and Complex Systems and Department of Mechanics and Engineering Science, Peking University, Beijing 100871, China

[2]Department of Basic Course, Naval University of Engineering, Wuhan 430043, China

[3]Department of Aerospace and Mechanical Engineering, University of Arizona, Tucson, AZ 85721, USA

[4]Department of Mathematics, University of California, Los Angeles, CA 90095, USA

(Received 7 December 2004 and in revised form 6 June 2006)

We have conducted a detailed analysis of scaling for longitudinal and transverse velocity structure functions in a turbulent free shear flow. The free shear flow is generated via a mixing layer under varying conditions of upstream flow disturbances. Two velocity components are simultaneously measured with a pair of cross-wires at two spanwise locations, with varying positions of the second cross-wire, which allows us to study the statistics of two longitudinal and four transverse velocity increments. Spectra, probability density functions of the velocity increments, and scaling exponents are measured and discussed in relation to flow structures such as streamwise and spanwise vortices. Scaling exponents of the velocity structure functions are interpreted in the phenomenological framework of the hierarchical structure (HS) model of She & Leveque (*Phys. Rev. Lett.* vol. 72, 1994, p. 336). One HS parameter (β) specifying similarity between weak and strong vortices is shown to be universal for all structure functions, and another HS parameter (γ) related to the singularity index of the so-called most intermittent structures shows strong dependence on flow structures. The strongest intermittency occurs in the form of streamwise vortices. The results confirm that coherent small-scale flow structures are responsible for intermittency effects and anomalous scaling, and a complete set of measurements of longitudinal and transverse velocity variations are required to derive flow structural information.

1. Introduction

Statistical analysis of shear-flow turbulence has recently attracted much attention (Gualtieri *et al.* 2002; Arimitsu & Arimitsu 2002; Fujisaka *et al.* 2002; Casciola *et al.* 2003; Jacob *et al.* 2004). There are at least two important motivations. First, turbulence in real flows is often generated by instabilities where shear is present. A typical example is the wall-bounded flow in a channel or the flow over a flat plate, where turbulence is produced near the wall with a strong shear and then migrates to another spatial location. Another example is a free shear flow in a mixing layer where a Kevin–Helmholtz-type instability generates spanwise vortices which subsequently

† Author to whom correspondence should be addressed: she@mech.pku.edu.cn

break down to produce turbulence. The fluid mechanical study of these two types of flow has yielded much quantitative knowledge about the mean flow and qualitative knowledge about flow structures (Cantwell 1981; Robinson 1991). However, in the fully developed turbulence regime, fluctuations are generated on a wide range of scales via complex cascade dynamics. The lack of detailed characterization of the properties of fluctuations makes it difficult to derive a self-consistent closure theory. Shear-flow turbulence is the simplest real-world turbulent system to build a bridge between the mean flow and fluctuation structures.

Secondly, the statistical physics has advanced considerably during the past two decades, and has proved helpful in understanding the scaling and intermittency property of homogeneous isotropic turbulence. When a cascade of energy takes place to produce fluctuations at small scales, non-uniformity of the energy flux leads to intermittency effects, strongly non-Gaussian statistics and anomalous scaling (She 1991; Sreenivasan & Antonia 1997). There is overwhelming evidence (Sreenivasan 1991) that velocity fluctuations in a turbulent flow display multifractal-type scaling (Frisch 1995; Mandelbrot 1974), and a simple phenomenology called hierarchical structure (HS) by She & Lévêque (1994) has proved to be capable of describing the scaling accurately (She 1998). We will refer to the original proposal of She & Lévêque (1994) as SL94, but will refer to its extension to more general situations where two parameters can be determined in specific flows as the HS model. A noteworthy feature of the HS model is that the parameters seem to have a physically sound interpretation. One parameter (β) describes how similar the fluctuation structures are with increasing intensities, and another parameter (γ) is related to the (scaling) property of the most intense fluctuation structures. The validity of the HS model has been established by the measurements in experiments (Ruiz-Chavarria, Baudet & Ciliberto 1994) and in numerical simulations (Cao, Chen & She 1996) of isotropic turbulence. It is intriguing to extend the analysis to real flow systems where non-trivial flow structures are present. Shear flow is a good point to start.

There have been many studies of shear-flow turbulent structures (see e.g. Adrian, Meinhart & Tomkins 2000; Rogers & Moin 1987; Lee, Kim & Moin 1990; Kida & Tanaka 1994). Earlier experimental studies on homogeneous shear flows by Champagne, Harris & Corrsin (1970) and Tavoularis & Corrsin (1981) emphasized the local isotropy of the small-scale fluctuations. This continues to inspire studies, e.g. by Pumir & Shraiman (1995) and Pumir (1996). From a statistical physics point of view, the local isotropy is a special self-organized quasi-equilibrium state of the homogeneous flow. Persistent anisotropy is a sign of strong deviation from the quasi-equilibrium state of homogeneous and isotropic turbulence. Discovering quantitative global measures for a far-from-equilibrium state has been a continuing effort in non-equilibrium statistical mechanics. Shear-flow turbulence is therefore a remarkable system for non-equilibrium statistical physics studies.

Toschi, Lévêque & Ruiz-Chavarria (2001) proposed an integral structure function (ISF) to account for the leading effects of shear intensity on the variation of scaling on phenomenological grounds. Gualtieri *et al.* (2002) and Casciola *et al.* (2003) established a new similarity law for shear-dominated turbulence in a boundary layer and in a homogeneous shear flow. The new similarity law extends the Kolmogorov refined similarity hypothesis (RSH) for homogeneous turbulent flows, and may be considered to be a form of the self-organization specific to turbulent shear flows. In addition, Gualtieri *et al.* (2002) reported the existence of a universal relative scaling of the energy dissipation fluctuations in homogeneous shear turbulence, identical to that in homogeneous isotropic turbulence. We believe that this is another form of the

self-organization laws for turbulence. An intriguing question investigated here is the nature of the universal relative scaling.

Whereas a homogeneous shear flow is translation-invariant in the vertical (shear) direction, a free shear flow in a mixing layer develops growing spanwise vortices in the downstream direction. The rate of shear is not constant in both the streamwise and vertical directions. However, in the symmetric middle plane of a mixing layer, we expect to observe a number of robust dynamical features of a homogeneous shear flow, particularly regarding the streamwise and spanwise variations. The present study is devoted to a detailed scaling analysis of velocity fluctuations in a free shear flow.

Specifically, we have conducted simultaneous measurements of two velocity components at two different spanwise locations by a pair of cross-wire probes, which allows examination of the velocity increments in both the streamwise (x) and spanwise (z) directions. By rotating the cross-wire probes, we obtain all three velocity components, which allows us to study two longitudinal velocity increments: $\delta_x u(\ell) = u(x+\ell) - u(x)$ and $\delta_z w(\ell) = w(z+\ell) - w(z)$, and four transverse velocity increments: $\delta_z u(\ell) = u(z+\ell) - u(z)$, $\delta_x v(\ell) = v(x+\ell) - v(x)$, $\delta_z v(\ell) = v(z+\ell) - v(z)$ and $\delta_x w(\ell) = w(x+\ell) - w(x)$. This rich set of data characterizes the development of fluctuation structures in terms of the statistics of velocity increments. Chen *et al.* (1997) established a generalized RSH which relates the transverse velocity increments to the vorticity fluctuation in isotropic turbulence. While the study of longitudinal versus transverse velocity structure functions continues to be an intriguing issue, our central theme here is to find statistical evidence of flow structures or to relate statistical measures of scaling to fluid dynamical mechanisms.

In order to quantify the role of flow structures for the explanation of the anomalous scaling of various velocity increments, we must select a phenomenological framework. Biferale *et al.* (2002) developed an analysis of turbulent fluctuation structures in a numerical channel flow in terms of SO(3) and SO(2) decomposition. Evidence of streak-like and hairpin structures can be extracted from the analysis. However, as Biferale *et al.* pointed out, we still need to understand the physics of anisotropic structure. This understanding would involve the quantitative description of the scaling exponents. The HS model is a particularly suitable framework in which to carry out this study. In this framework, turbulence is considered to be a hierarchy of complex flow patterns, rather than fluctuations randomly assembled. The basic assumption of the HS model is that the sequence of fluctuations of increasing intensity satisfy a generalized hierarchical similarity law rather than the Kolmogorov's complete scale similarity law. Hierarchical similarity seems to be a universal self-organizational principle, and a parameter β gives quantitative characterization of the degree of the self-organization. On the other hand, the so-called most intermittent structures are characteristic of intense flow structures (as seen in the Couette–Taylor flow, She *et al.* 2001) which are believed to be related to the non-universal aspects of turbulence. The free shear-flow measurement in this work provides an example for an empirical study of both the universal HS similarity and the non-universal properties of the most intermittent structures (in streamwise and spanwise directions). To our knowledge, this is the first attempt to establish a relationship between the values of the HS parameters (β and γ) and the properties of flow structures in a concrete flow system, which may provide a foundation for further development of sound theoretical concepts.

The paper is organized as follows. In § 2, we give a self-contained description of the HS phenomenology and its possible application into the real turbulent flows. In particular, we present the method of the HS analysis, namely the β-test and the γ-test, and explain the interpretations of the two fundamental parameters. Section 3

introduces the experimental set-up and describes the flow conditions that give rise to the data studied in this work. In § 4, we present results of our analysis on spectra, probability density functions (PDFs), scaling and HS parameters. Finally, we offer a summary and some additional discussion in § 5.

2. The HS description

Under the assumption of local isotropy, Kolmogorov (1941, hereinafter referred to as K41) proposed that the velocity structure functions $S_p(\ell) \equiv \langle |\delta v_\ell|^p \rangle$ have simple power-law dependence on ℓ within the inertial subrange

$$S_p(\ell) \sim \epsilon^{p/3} \ell^{p/3}. \tag{2.1}$$

This power-law $p/3$ is an indication of a universal behaviour of small-scale fluctuations. Later, both experimental measurements and computer simulations (Frisch 1995) have established that the power-law scaling exists in the inertial range, but the scaling exponents are different from $p/3$, namely,

$$S_p(\ell) \sim \ell^{\zeta_p}, \tag{2.2}$$

and ζ_p has a nonlinear dependence on p. The so-called anomalous scalings ζ_p are also known as intermittent effects since the higher-intensity fluctuation events of δv_ℓ are expected at small scales compared to the normal scaling situation.

Later a more general scaling relation called the extended self-similarity (ESS) (Benzi *et al.* 1993) property of turbulence was introduced to describe the scaling behaviour of the higher-order moments. Such a scaling property has the form:

$$S_p(\ell) = S_q(\ell)^{\zeta_{p,q}}, \tag{2.3}$$

where $\zeta_{p,q}$ are called relative scaling exponents. The ESS extends the scaling in physical scales to a relative scaling between the velocity structure functions at two different orders p and q. Benzi *et al.* (1996) reported the experimental evidence of a generalized ESS property (GESS) satisfied by flows with a variety of physical conditions where the ESS property is not well satisfied. GESS has the form:

$$G_{(p,q)}(\ell) \propto G_{(p',q')}(\ell)^{\rho(p,q;p',q')}, \tag{2.4}$$

where $G_{(p,q)}(\ell)$ is the dimensionless structure function:

$$G_{(p,q)}(\ell) = S_p(\ell)/S_q(\ell)^{p/q}. \tag{2.5}$$

Usually we set $q = q' = 3$ when calculating G-function: $G_p(\ell) = S_p(\ell)/S_3(\ell)^{p/3}$.

Both ESS and GESS indicate the possible existence of other self-similarity properties in turbulence which persist even when the scale similarity does not hold. In some sense, the new scaling relations reveal more fundamental scaling properties of turbulence than the original inertial-range scaling of K41. The HS model was originally proposed (She & Lévêque 1994) to understand the deviation of scaling from K41. In this work, most HS analysis is carried out with respect to the ESS scaling.

The key point in the HS model is the introduction of a hierarchy of moment ratios, namely

$$F_p(\ell) = \frac{S_{p+1}(\ell)}{S_p(\ell)}, \tag{2.6}$$

each of which has the dimension of δv_ℓ. Hence, $F_p(\ell)$ is the amplitude of the fluctuations which may be characteristic of the turbulent field. It has been verified

with both experimental and numerical data (Liu & She 2003; She & Liu 2003) that $F_p(\ell)$ increases monotonically with p and hence characterizes fluctuation structures of increasing intensities. We refer to $F_p(\ell)$ as the pth-order HS function.

An intuitive idea behind the HS model is that a self-organized dynamical state of turbulence is characterized by a similar dependence of $F_p(\ell)$ on ℓ for different values of $p(0 \leqslant p \leqslant \infty)$. In terms of scaling law, the simplest similarity property is that all $F_p(\ell)$ have the same scaling. This gives rise to the K41 theory of turbulence for which ζ_p has a linear dependence on p. It can be shown that a complete self-similarity is ensured in this case and small- and large-amplitude fluctuations have exactly the same dependence on ℓ. This complete self-similarity law has been demonstrated to be invalid in experiments and by numerical simulations, and the dissipation fluctuations have anomalous scalings in ℓ (Sreenivasan 1991).

The HS model postulated that the most intense structures $F_\infty(\ell) = \lim_{p\to\infty} F_p(\ell)$ play a special role in defining the dynamical state of turbulence, and all other fluctuation structures of finite p obey a hierarchical similarity law, namely:

$$\frac{F_{p+1}(\ell)}{F_\infty(\ell)} = A_p \left(\frac{F_p(\ell)}{F_\infty(\ell)}\right)^\beta, \tag{2.7}$$

where $0 \leqslant \beta \leqslant 1$, A_p are independent of ℓ. We may proceed to define a method of analysis which does not involve the hypothetical quantity $F_\infty(\ell)$, by considering the ratio

$$\frac{F_{p+1}(\ell)}{F_2(\ell)} = \frac{A_p}{A_1} \left(\frac{F_p(\ell)}{F_1(\ell)}\right)^\beta. \tag{2.8}$$

Both sides of (2.8) can be computed from any empirical PDFs (or histograms) of δv_ℓ calculated from an experimental or numerical turbulent fluctuation field. The linearity in the log–log plot of (2.8) can be a direct test of the validity of (2.7) and the slope β can be measured. This will be referred to as the HS similarity test, or β-test (She *et al.* 2001; Liu & She 2003; She & Liu 2003).

Furthermore, She (1998) has shown that (2.7) implies a general formula for relative scaling exponents which is also known as extended self-similarity (ESS) scaling (Benzi *et al.* 1993), given by

$$\zeta_p = \gamma p + (1 - 3\gamma)\frac{1 - \beta^p}{1 - \beta^3}, \tag{2.9}$$

where $\zeta_3 = 1$ and the parameter γ is defined by $F_\infty(l) \sim l^\gamma$ where $F_\infty(l)$ represents the amplitude of the most intermittent structure. Then, a simple algebraic manipulation gives

$$\zeta_p - \chi(p;\beta) = \gamma(p - 3\chi(p;\beta)), \tag{2.10}$$

where $\chi(p;\beta) = (1 - \beta^p)/(1 - \beta^3)$. When we plot $\zeta_p - \chi(p;\beta)$ *vs.* $p - 3\chi(p;\beta)$, the slope obtained is the parameter γ. This process is referred to as the γ-test (She *et al.* 2001; Liu & She 2003; She & Liu 2003).

The HS model gives a concise description of the set of multi-scale and multi-intensity properties. It seems to be generally applicable to many statistically stationary multi-scale fluctuation fields generated from strong nonlinear interactions. Indeed, it has been discovered that the HS similarity is satisfied in a variety of nonlinear systems and other complex systems, such as the Rayleigh–Bénard convection (Ching & Kwok 2000; Ching *et al.* 2003), the Couette–Taylor flow (She *et al.* 2001), flows in a rapidly rotating annulus (Baroud *et al.* 2003), the passive scalar fields (Lévêque *et al.* 1999), the climate variations (She *et al.* 2002), the variation of nucleotide density along DNA

sequences (Ouyang & She 2004), the diffusion-limited aggregates (Queiros-Conde 1997), and a fluctuating luminosity field of natural images (Turiel *et al.* 1998).

The meaning of the parameter β (She 1998; She *et al.* 2001) can be readily obtained from (2.7), which describes how similar the two successive HS functions F_{p+1} and F_p are. When β approaches 1, high $(p+1)$ HS function is like low (p) HS function; in other words, strong and weak fluctuation structures are alike. This can be realized at either an extremely ordered state or a completely homogeneous disordered state. In the former, the structures of various intensities are strongly correlated and hence behave similarly at different length scales. This is observed in Belousov–Zhabotinsky reaction systems and in numerically simulated complex Ginzberg–Landau equations (Guo *et al.* 2003; Liu *et al.* 2003, 2004). The other situation corresponds to the hypothetical field postulated by the K41 theory with complete self-similarity; unfortunately, it has not yet been observed in real physical systems. Another extreme case is the limit $\beta \to 0$. This is the case in which $F_\infty(\ell)$ stands out as the only singular structures which are responsible for the physical process. A mathematical model displaying the dynamics of one-dimensional shocks, the so-called Burgers equation, exhibits behaviour close to this situation, where only shocks at isolated points are responsible for the energy dissipation and all statistical moments are determined by the discontinuities across the shocks (She, Aurell, & Frisch 1992).

The empirical study of experimental turbulence reveals that in realistic turbulent systems, $0 < \beta < 1$, namely the most intense fluctuations do not completely dominate, nor are the fluctuation structures of various intensities completely alike. The fluctuation structures of various intensities are all responsible for the physical process, but they are related by the hierarchical similarity law (equation (2.7)) that we believe is a form of self-organization in the system. In particular, if the velocity structure function δv_ℓ is replaced by the dissipation ε_ℓ at the scale ℓ, β measures the degree of the efficiency of energy transfer from scale to scale.

In a study applying the HS analysis to ordered spiral patterns and disordered spatio-temporal chaos, Liu *et al.* (2004) has shown that the parameter β gives a quantitative description of the degree of order/disorder and of homogeneity/heterogeneity of two-dimensional fields. For β close to one, the system appears to be orderly homogeneous with uniformly distributed structures; at smaller β the system contains a mixture of order/disorder and appears to be heterogeneous with the development of the overwhelmingly disordered and intermittent spatiotemporal state. In addition, it was discovered that the measured HS parameter β acts as an order parameter that can give a quantitative description of the transition from order state (spiral wave) to disorder state (spiral turbulence), and from one kind of spiral turbulence state to another. These findings further motivate the present study of the hierarchical structures in fully developed turbulent flows and detailed examination of the nature of β.

While the parameter β indicates a global property of self-organization of the system, the parameter γ measures how singular the most intermittent structure is. By definition, $F_\infty(\ell) \sim \ell^\gamma$, hence it is a property of very high-order moments $p \to \infty$. The smaller γ is, the more singular the most intermittent structure appears. Although γ is, theoretically speaking, a property of very high-order moments, we find in analysis of experiments that on a modest range of p $(3 \leqslant p \leqslant 6)$ we can define the most intermittent structures. This is because the structures that contribute to $F_p(\ell)$ for $3 \leqslant p \leqslant 6$ comprise most of the intensive fluctuations that are statistically significant. The term γ is characteristic of those structures in the finite (but long) velocity record.

The most intermittent structure may be high-intensity vortices or other localized flow structures such as strong streamwise and spanwise vortices in the present free

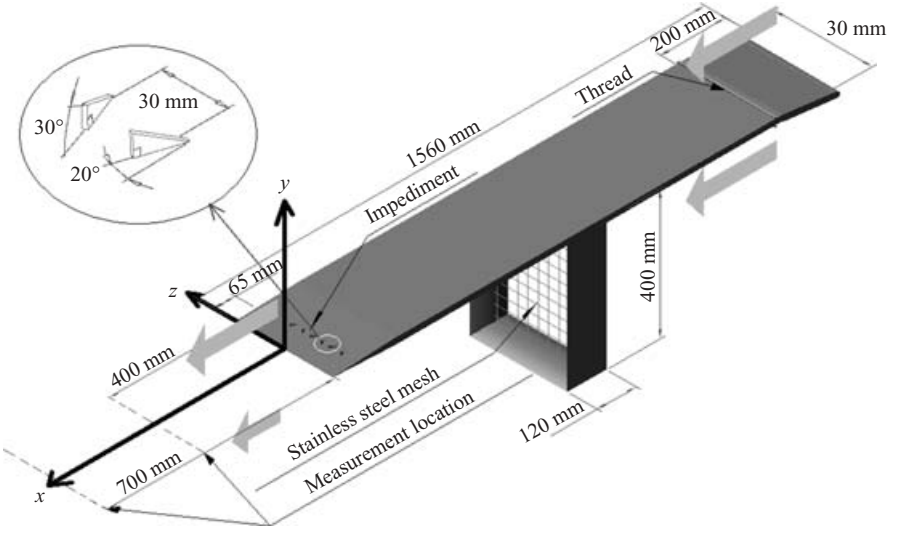

FIGURE 1. Sketch of the experimental set-up. Note the presence of several impediments for the generation of spanwise disturbances.

shear flow. Hence, γ may be a measure sensitive to the local turbulent environment in question. Previous study of the hierarchical structures in the Couette–Taylor flow (She *et al.* 2001) has shown that β is independent of the Reynolds number, whereas γ shows a transition corresponding to the breaking down of the Taylor vortex. It was thus hoped that the HS analysis would shed light on the properties of the shear flow and other inhomogeneous turbulence fields displaying temporal, spatial or spatiotemporal coherent structures.

3. Experimental set-up

Our experiments were conducted in the low-turbulence wind tunnel in the State Key Laboratory for Turbulence and Complex Systems (LTCS) at the Peking University, with a test section of 0.8 m high, 0.3 m wide and 3.2 m long. The wind tunnel can generate a uniform flow with a maximum air speed of $23\,\mathrm{m\,s^{-1}}$ and a residual turbulence level of 0.085 %. A flat split plate of 0.300 m wide, 1.558 m long and 17 mm thick was inserted into the test section (figure 1). The streamwise, the vertical and the spanwise directions are denoted by x, y and z, respectively.

The flat plate separated the incoming flow into two layers, and the flow below the plate passed through a filter that reduced its speed and formed a mixing layer at the end of the plate. A leading-edge flap was applied to avoid leading-edge separation (see figure 1). A trip wire was placed upstream as an artificial transition device. In addition, a spanwise row of impediments was installed close to the trailing edge of the split plate to enhance lateral velocity fluctuations when needed. The impediments was essentially a set of small vortex generators that were arranged to produce counter-rotating streamwise vortex pairs (see figure 1).

Two sets of experiments were carried out with and without impediments, which will be referred to as exp. I and exp. II, respectively. During both experiments, the incoming velocity was about 9–$11\,\mathrm{m\,s^{-1}}$. Before taking long time series data for the HS scaling analysis, the mean velocity, turbulence energy and Reynolds stress distributions were measured as a background check. A set of mean velocity profiles

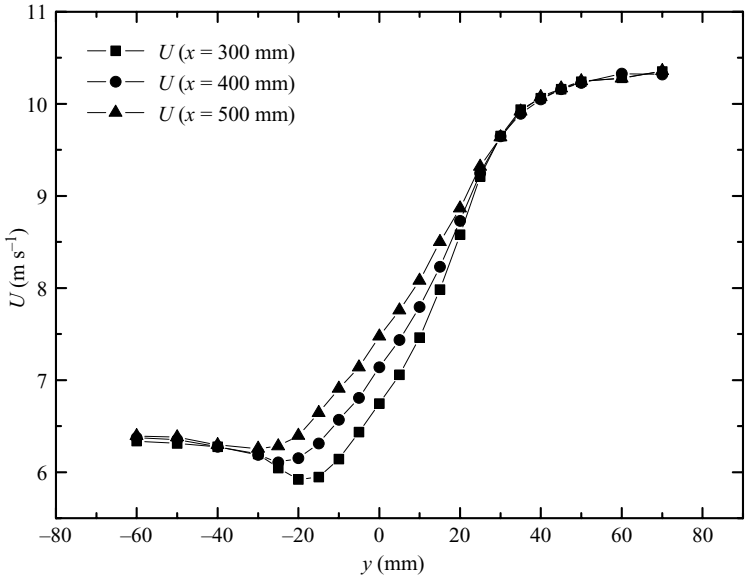

FIGURE 2. The mean velocity profiles measured at the centre of the channel ($z = 0$) and at several downstream positions in exp. II (with impediments). Note that the long series of velocity data analysed in this paper are obtained at $y = 0$.

in the mixing layer region with impediments are shown in figure 2. The long time series data are later collected at $y = 0$ at several downstream locations (400 mm and 700 mm). Persistent mean shear is present at these locations, as seen from figure 2.

Cross-wire probes were applied for simultaneous measurements of u, v or u, w velocity components in the mixing region to obtain long time series of velocity signals for conducting statistical analysis. Each measurement contains about 7.2×10^7 samples (40 min recording with a sampling frequency of 48 kHz). The measurements were made simultaneously at two spanwise locations. Both cross-wire probes were placed on the $y = 0$ plane, parallel to each other, where one of them (referred to as probe c1) was fixed at the centre and the other (referred to as probe b2) recorded data at locations with a series of spanwise spacings Z relative to its partner. To analyse the streamwise velocity structure functions, the Taylor frozen hypothesis was employed to convert the temporal fluctuations to streamwise fluctuations in the x-direction. Then, in addition to the spatial variation in z and with three velocity components, we constructed two longitudinal and four transverse velocity increment statistics. This gave us a rich set of data for the study of the fluctuation structures in the free shear turbulence.

In the present work, we have analysed three groups of experimental data, which are (*a*) 40*p*, obtained at 400 mm downstream without applying the impediments; (*b*) 40*e*, with impediments at 400 mm; and (*c*) 70*e*, with impediments at 700 mm. The basic flow parameters in these modest-Reynolds-number free-shear-flow experiments is given in table 1. The term ϵ was determined from the relation $\epsilon = 15(\nu/U^2)\langle(\partial_t u)^2\rangle$ where u (or v, or w) is the r.m.s. velocity fluctuation and U is the mean streamwise velocity. Other quantities (ℓ_0, λ, η, R_λ and R_0) were evaluated accordingly. Note that all length scales in table 1 are derived from the Taylor hypothesis, so they only describe properties of fluctuation structures in the streamwise direction. Inspection of these parameters indicates that our free shear flow and moderate-Reynolds-number

Flow parameters	40*p*	40*e*	70*e*
U (m s^{-1})	10.28	9.92	9.78
$\langle u^2\rangle$ (m^2 s^{-2})	1.29	1.31	0.71
$\langle v^2\rangle$ (m^2 s^{-2})	0.56	0.67	0.40
$\langle w^2\rangle$ (m^2 s^{-2})	0.62	0.74	0.50
$\langle u^2\rangle^{1/2}/\langle U\rangle$ (%)	11.06	11.53	8.60
$\epsilon^u = 15(\nu/U^2)\langle(\partial_t u)^2\rangle$ (m^2 s^{-3})	26.25	32.63	38.80
$\epsilon^v = 15(\nu/U^2)\langle(\partial_t v)^2\rangle$ (m^2 s^{-3})	33.25	42.83	23.54
$\epsilon^w = 15(\nu/U^2)\langle(\partial_t w)^2\rangle$ (m^2 s^{-3})	32.19	42.01	25.61
$\ell_0^u = \langle u^2\rangle^{3/2}/\epsilon^u$ (mm)	56.1	46.2	15.3
$\ell_0^v = \langle v^2\rangle^{3/2}/\epsilon^v$ (mm)	12.5	13.1	10.9
$\ell_0^w = \langle w^2\rangle^{3/2}/\epsilon^w$ (mm)	15.2	15.3	13.9
$\lambda^u = [U^2\langle u^2\rangle/\langle(\partial_t u)^2\rangle]^{1/2}$ (mm)	3.43	3.09	2.08
$\lambda^v = [U^2\langle v^2\rangle/\langle(\partial_t v)^2\rangle]^{1/2}$ (mm)	1.99	1.94	2.02
$\lambda^w = [U^2\langle w^2\rangle/\langle(\partial_t w)^2\rangle]^{1/2}$ (mm)	2.14	2.05	2.16
$\eta^u = (\nu^3/\epsilon^u)^{1/4}$ (mm)	0.11	0.11	0.10
$\eta^v = (\nu^3/\epsilon^v)^{1/4}$ (mm)	0.11	0.10	0.11
$\eta^w = (\nu^3/\epsilon^w)^{1/4}$ (mm)	0.11	0.10	0.11
$R_\lambda^u = \langle u^2\rangle^{1/2}\lambda^u/\nu$	245	223	110
$R_\lambda^v = \langle v^2\rangle^{1/2}\lambda^v/\nu$	94	101	80
$R_\lambda^w = \langle w^2\rangle^{1/2}\lambda^w/\nu$	106	112	96
$R_0^u = \langle u^2\rangle^{1/2}\ell_0^u/\nu$	4026	3342	813
$R_0^v = \langle v^2\rangle^{1/2}\ell_0^v/\nu$	590	678	434
$R_0^w = \langle w^2\rangle^{1/2}\ell_0^w/\nu$	756	834	619

TABLE 1. Flow parameters estimated based on streamwise velocity fluctuation signals for the free shear flows studied in the experiments. Taylor's hypothesis is employed. The kinematic viscosity is $\nu = 1.5 \times 10^{-5}$ m^2 s^{-1}.

turbulence are properly generated. The Kolmogorov dissipation length scale η is quite constant ($\eta \approx 0.11$) for all three velocity components in all three flow conditions; the difference of their Reynolds numbers is due to the difference in the integral length scales used for calculations below.

From figure 2 and table 1, it is clear that we have generated a set of free shear flows with rich turbulent fluctuations, which are different from a standard mixing layer. Because of the presence of upstream turbulence-generation mechanisms, the turbulence intensity and the Reynolds numbers depend on streamwise and spanwise positions, hence strong spanwise and streamwise vortices actively evolve in the downstream direction. We stress that the purpose of the present work is to study scaling behaviour of turbulence in a free shear flow for establishing possible correlation between the relative scaling and turbulent flow structures. This is difficult and requires more experimental work. We believe that the assumption about the universal nature of intermittency effects is not correct and the deviations of the scaling parameters reflect the varying properties of the intense fluctuation structures. We are convinced that the present experimental set-up, although simpler than the traditional high-standard mixing-layer generator, is appropriate for the investigation of the influence of various intermittent structures (with the presence of impediments) on the abnormal scaling. Note that the choice of high sampling frequency (48 kHz) is also essential in the present study in order to resolve the small scales.

The mean velocity profiles of U in figure 2 allow us to estimate the mean shear rate and the shear length scale. One estimate of the shear length scale is by

$(U_1 - U_2)/(\mathrm{d}U/\mathrm{d}y)$, which gives a scale of approximately 30 to 70 mm; another estimate is $\sqrt{\epsilon/S^3}$ where ϵ is the mean dissipation rate and S is the local shear rate. Using flow parameters in table 1, the latter estimate gives a shear length scale between 5 and 10 mm depending on the location of the measurement, and it is more relevant to the fluctuation scales, and hence should be used to compare to the scales of the scaling range discussed below. Since the shear scales are between ℓ_0 and η, the analysis of the relative scaling conducted below reveals the anisotropic effects of flow structures due to the shear, hence the present correlation study between the scaling and flow structure is meaningful.

4. Results

The present study is devoted to the analysis of the velocity fluctuation structures in free shear flow turbulence. We will examine PDFs of velocity increments, spectra, and scaling properties of both longitudinal and transverse velocity increments of all three components. We report the major results in the following section.

4.1. *Qualitative behaviour: signals and probability density functions*

First, we attempt to give a global view about the fluctuation structures in the free shear flow. Figure 3 shows typical velocity signals measured in the three conditions $40p$, $40e$ and $70e$. It can be seen that the fluctuations of v and w components are less developed than the u component, especially in the case of $70e$, which is consistent with the values of $\langle u^2 \rangle$, $\langle v^2 \rangle$ and $\langle w^2 \rangle$ reported in table 1. The component u contains notably larger-scale structures than v and w, which is also consistent with larger ℓ_0 reported in table 1. These signals describe only streamwise fluctuation structures, so there is no visible difference between the fluctuations with or without impediment (comparing $40p$ with $40e$). However, the decay of fluctuation structures can still be visible comparing $40e$ with $70e$. In the past, turbulent velocity signals reported in the literature tend to reveal the random nature of the fluctuations; we would like to emphasize its complex nature and attempt to associate them with varying scaling measurement.

Energy spectra reported in figure 4 give a quick view of the distribution of energy at different scales (in the streamwise direction under Taylor's hypothesis) for different velocity components. Both probes show consistent energy distributions across scales, and the component u displays much stronger motion at large scales than v or w, but have similar energy distribution at small scales. Compensated energy spectra are also shown in figure 4 indicating the existence of a short inertial range ($R_\lambda = 237$, see table 1). Inspection shows that unlike u, the vertical and spanwise velocity v and w have an energy spectrum with a slope less than $-5/3$. It is seen from the spectra in figure 4 that all three velocity components have a moderate scaling range ($0.03\eta < k < 0.2\eta$). Note that we have used a different dissipation length scale (see table 1) for different spectra. In anisotropic turbulence at finite Reynolds number, the small-scale eddies are unlikely to be isotropic, especially in a strong shear layer where there are strong interactions between coherent and random structures (Melander & Hussain 1993). Hence, a unique Kolmogorov dissipation length scale is not adequate in anisotropic turbulence. We believe that each fluctuation spectrum should define its own characteristic length scale using the total dissipation rate calculated from the integral of $k^2 E(k)$. Observe that the three spectra do not collapse even at large wavenumbers, which is evidence of the anisotropy at small scales; a similar result was observed by Zhou, Heine & Wygnanski (1996).

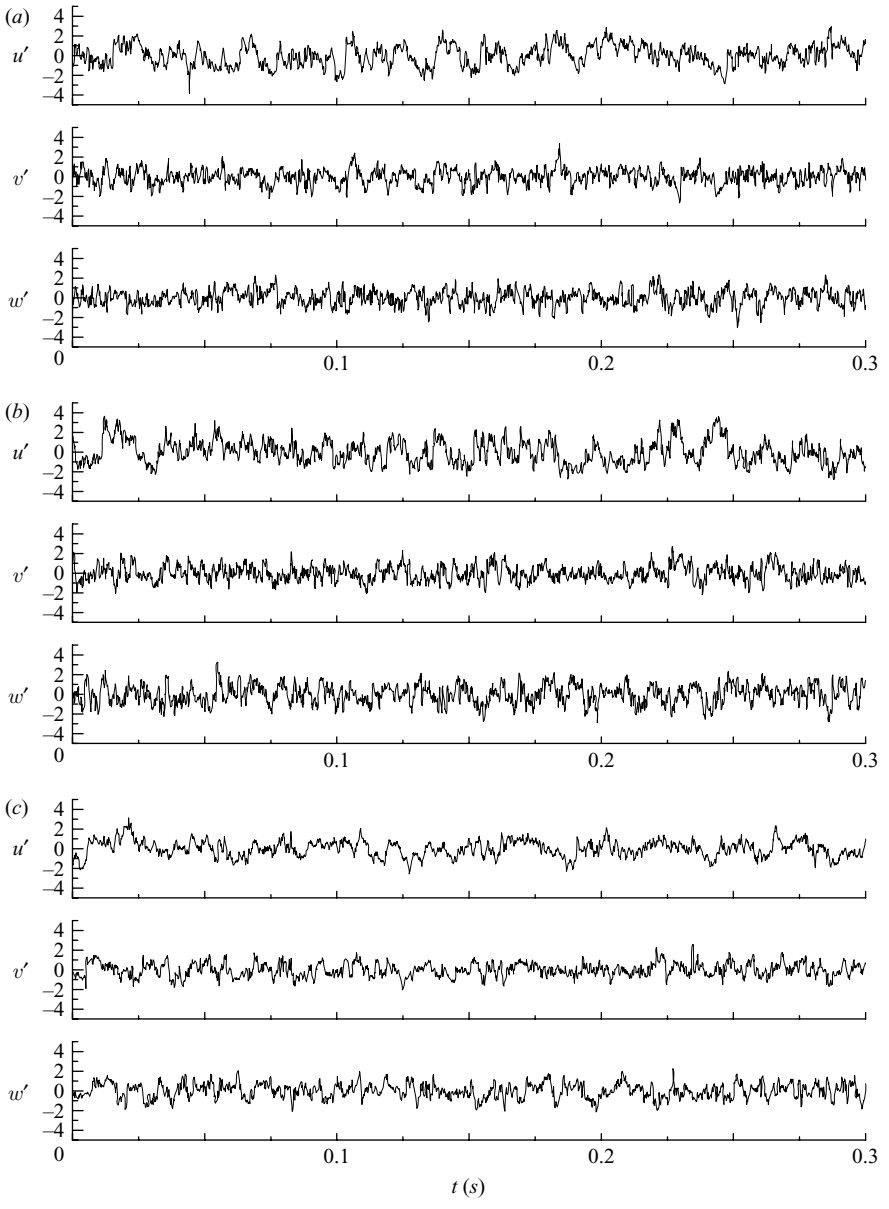

FIGURE 3. Typical velocity signals recorded under three flow conditions of the experiment. (*a*) 40*p*; (*b*) 40*e*; (*c*) 70*e*. The velocity signals are a kind of one-dimensional 'visualization' of flow structures, which contain such information as typical large-scale fluctuation patterns, the frequency of abrupt bursting events, etc. They are pertinent to the scaling analysis in this work which aims at revealing correlation structures across scales.

Saddoughi & Veeravalli (1994) have conducted measurements of longitudinal and transverse velocity fluctuations in a high-Reynolds-number boundary-layer experiment ($R_\lambda \sim 1450$), and found a significant difference between the scaling ranges for the two types of fluctuation. In particular, they found that the v spectrum is slightly flatter than the u spectrum, or the transverse velocity structure function has a smaller scaling exponent than the longitudinal one. Sreenivasan (1996) provides a

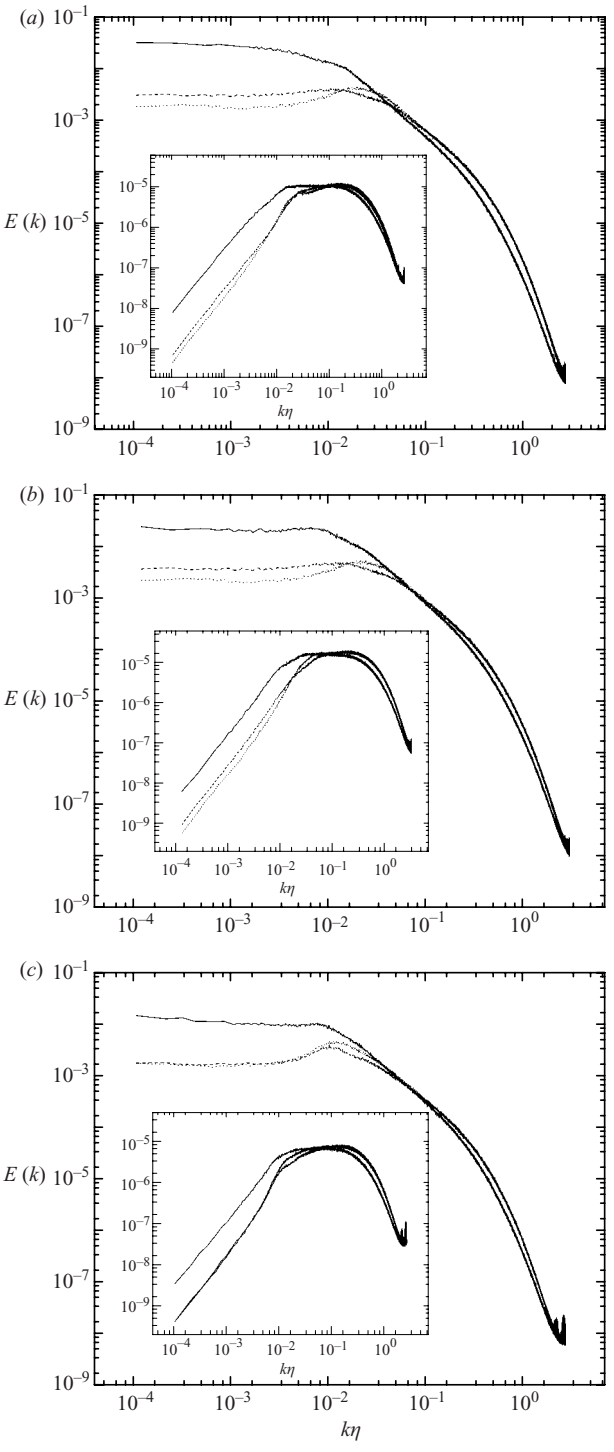

FIGURE 4. The typical energy spectra of longitudinal velocity u (solid line), vertical velocity v (dashed line) and transverse velocity w (dotted line) measured by the central probe under three flow conditions: (*a*) 40*p*, (*b*) 40*e* (*c*) 70*e*. Compensated spectra $E(k)(k\eta)^{5/3}$ for the same data are shown in insets.

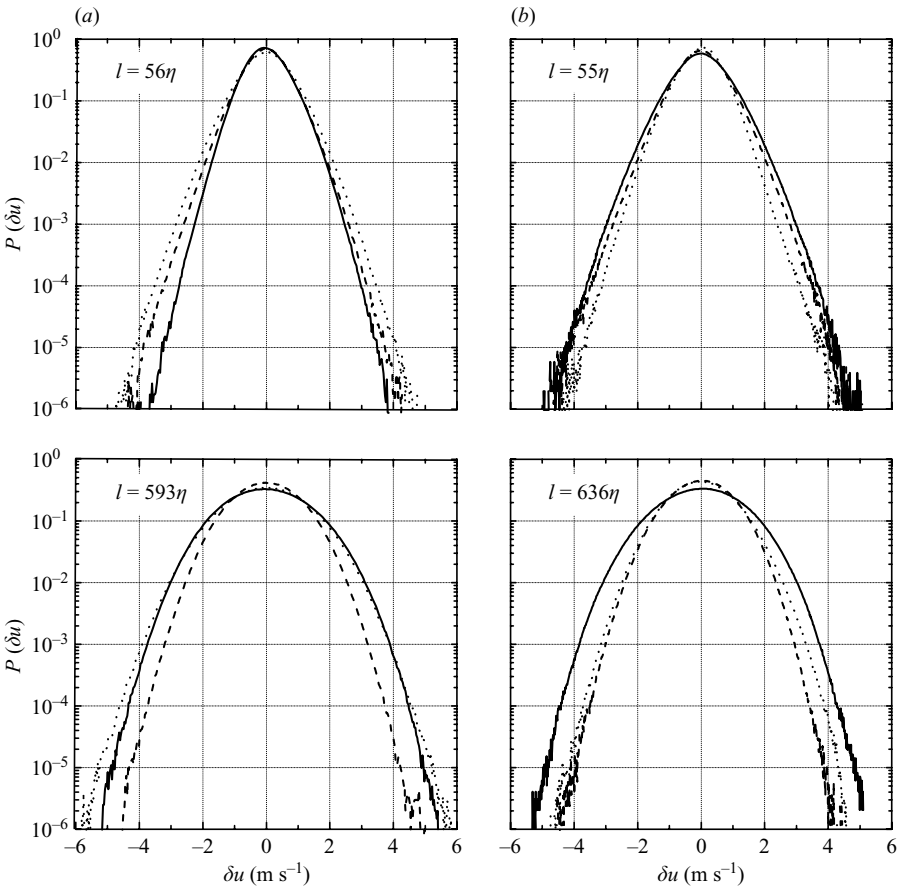

FIGURE 5. Longitudinal and transverse PDFs of velocity increments for three velocity components measured at 70*e*. (*a*) Streamwise increment in x; (*b*) spanwise increment in z, at two different scales ℓ in units of the Kolmogorov length scale $\eta \equiv 0.11$. Solid lines correspond to $\delta_x u$ and $\delta_z u$; dashed lines to $\delta_x v$ and $\delta_z v$; dotted lines to $\delta_x w$ and $\delta_z w$.

compilation of different flows and shows also that the v spectrum tends to be flatter than the u spectrum at moderate Reynolds numbers, and approaches to a Kolmogorov spectrum at very high Reynolds numbers ($R_\lambda \sim 3000$). Mydlarski & Warhaft (1996) also found in decaying grid turbulence that the v spectrum approximates more slowly with increasing R_λ to the $-5/3$ exponent than does the u spectrum. It is not yet fully understood why the longitudinal velocity component possesses a Kolmogorov spectrum at far lower Reynolds numbers than transverse components (see discussions in Sreenivasan 1996), but these results are consistent with our results reported above. In our case, v and w have less developed large-scale motions and smaller R_λ, which contributes also to flatter energy spectra.

A quick glance at probability density functions (PDFs) of various velocity increments gives insight into the development of fluctuation structures, especially of high intensities. A few typical PDFs of the six velocity increments at two different scales are displayed in figure 5. The transverse velocity increment PDFs have been calculated from two simultaneous measurements at two separate spanwise locations; the falling tails of these PDFs prove that the calculation is reasonably accurate.

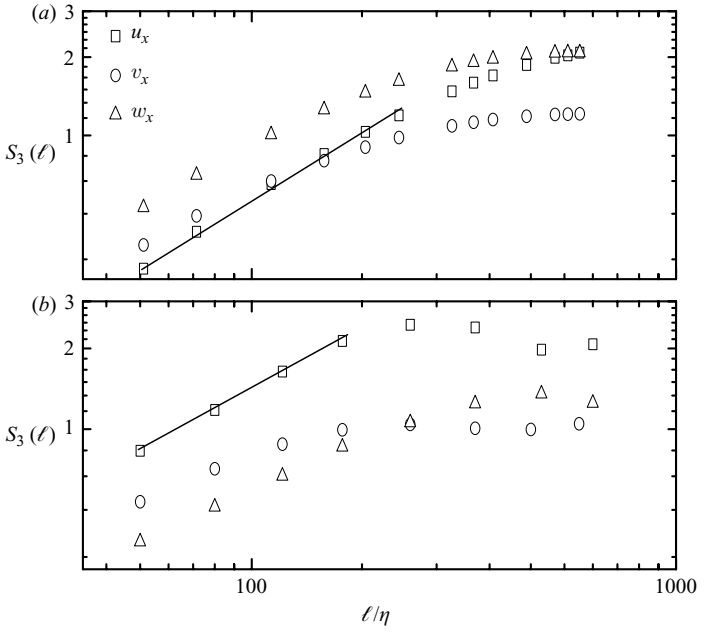

FIGURE 6. The third-order velocity structure function $S_3(\ell)$ in (a) the streamwise (x) direction and (b) the spanwise (z) direction as functions of the length scale ℓ/η with the data sets 70e. The solid line is $\sim \ell$.

4.2. *Scaling exponents*

In the past, the studies of anomalous scaling in turbulence have been mostly focused on longitudinal structure functions because they are associated with energy transfer and because they are easy to measure in experiments. More recent studies have been focused on both transverse and longitudinal velocity structure functions. There is considerable experimental evidence (Camussi & Benzi 1997; Dhruva, Tsuji & Sreenivasan 1997; Shen & Warhaft 2002) and numerical evidence (Boratav & Pelz 1997; Chen *et al.* 1997; Toschi *et al.* 1999; Chen *et al.* 2003) that the longitudinal scaling exponents are not equal to the transverse scaling exponents, especially in the turbulence at moderate Reynolds numbers. As the order p increases, especially when $p > 3$, the transverse scaling exponents are significantly smaller than the longitudinal ones. This observation introduces additional complexity in the phenomenology of small-scale turbulence, and is a challenge to the scaling theory.

In laboratory flows with shear, there is no established relation between scaling exponents of various transverse and longitudinal structure functions. The principal objectives of this work are to examine the scaling behaviours of these structure functions, and to derive as much information about the underlying flow structures as possible.

In figure 6, we plot the third-order longitudinal and transverse velocity structure functions $S_3(\ell)$ for various length scales in both streamwise and spanwise directions, in order to locate relevant physical scales for an inertial range. Because of the limited Reynolds number ($R_\lambda = 237$), only the u component displays a narrow linear range in the log–log plot for both x and z variations, implying an established constant energy flux in the streamwise velocity fluctuations. The other two velocity components have more complex interactions, giving rise to smaller amplitude and smaller rate of

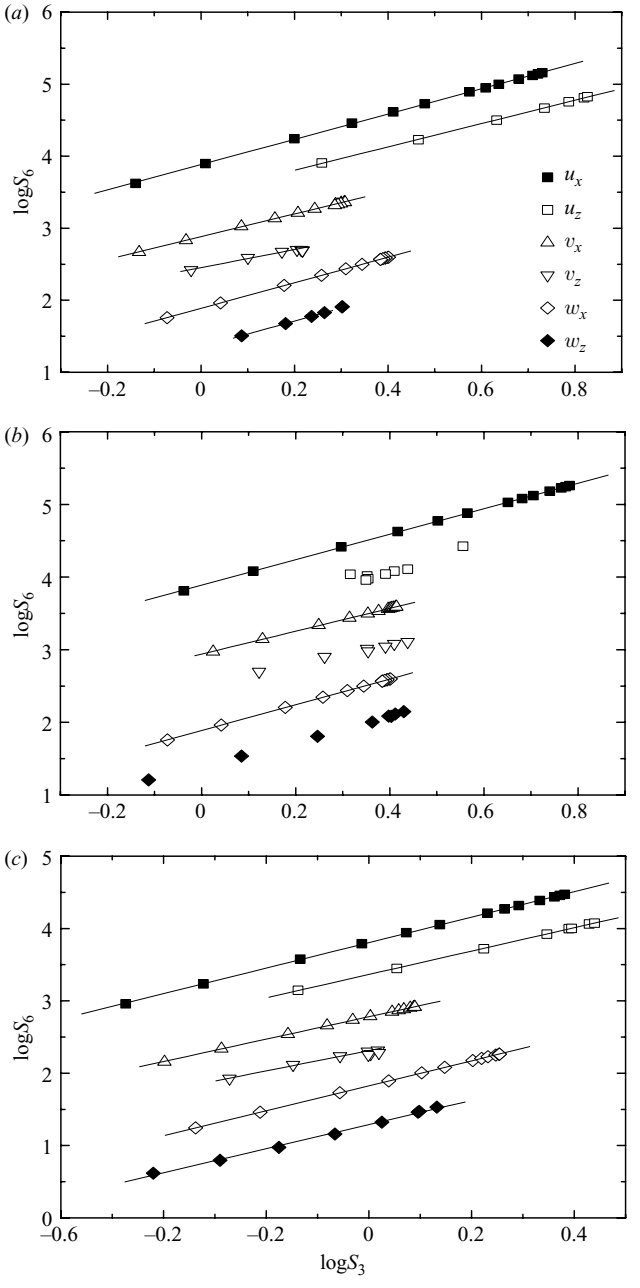

FIGURE 7. An illustration of the ESS plots ($\log S_3$ *vs.* $\log S_6$) for longitudinal (filled symbols) and transverse (open symbols) velocity structure function of u, v and w, respectively, under three flow conditions (*a*) 40*p*, (*b*) 40*e* (*c*) 70*e*. The lines are arbitrarily shifted for clarity.

change in ℓ of the third-order velocity structure function, which is the evidence of more singular structures (see below).

Hereinafter, we turn to discussions of ESS scaling property for longitudinal and transverse structure functions. The ESS plots (e.g. *p*th-order moments versus the third-order moment) are shown in figure 7 for all three sets of data, which allows

a comparison between them. Clearly, the ESS property is observed for both the longitudinal and transverse velocity increments of all three components of the velocity fields in all experimental data sets. These plots define an ESS scaling range for structure functions up to moment $p = 8$ for x-increments and to moment $p = 6$ for z-increments. Close inspection shows that the ESS property is valid in a narrower range $55\eta \leqslant \ell \leqslant 236\eta$ for z-increments, but in a wider rang $59\eta \leqslant \ell \leqslant 627\eta$ for x-increments. These ranges are consistent with the physical dimension of our experiment. Since $\eta \approx 0.1$ mm, the wavelength of the impediment is about 25 mm which is very close to the upper limit for the spanwise scaling range (236η). On the other hand, the upper limit of the streamwise scaling range is determined by the scale of the spanwise vortices which is the order of the mixing-layer thickness, around 80 mm in this experiment (compared to 627η).

Note that the shear scales estimated in the previous section (around 5–10 mm) are near the bottom of our scaling range, therefore the anisotropic effects of flow structures in the relative scaling are significant. This shows that the present analysis about the dependence of scaling parameters are meaningful for characterizing flow structures in the free shear flow.

The relative scaling exponents obtained by a least-squares fit of the ESS plots are given in table 3 and plotted in figure 8 together with the HS model and K41 models, where the two longitudinal scaling ($\zeta_p^{u,x}$, $\zeta_p^{w,z}$) and the four transverse scaling ($\zeta_p^{u,z}$, $\zeta_p^{v,x}$, $\zeta_p^{v,z}$, $\zeta_p^{w,x}$) exponents are all included. The consistency check of all three relative scaling exponents in x-increments are carried out with independent data sets of the simultaneous measurement by the two cross-wire probes ($c1$ and $b2$) and at different ΔZ-locations. They show small fluctuations within a few per cent.

A comparison of our results in a free shear flow with previous measurements is important to establish the credibility of the present measurement. Chosen for comparison are several measurements including a simulated Navier–Stokes isotropic turbulence by Chen *et al.* (1997), a homogeneous shear turbulence measurement by Shen & Warhaft (2002), a cylinder wake flow result by Bi & Wei (2003), and a high-resolution (up to $N = 1024^3$) numerical turbulence by Gotoh, Fukayama & Nakano (2002). Table 2 summarizes the results of both $\zeta_p^{u,x}$ and $\zeta_p^{u,z}$ in the five measurements (except in Shen & Warhaft 2002, $\zeta_p^{u,y}$ is reported instead of $\zeta_p^{u,z}$ and a conversion to ESS exponents is made here). Our results are consistent with the results of Chen *et al.* (1997), Shen & Warhaft (2002) and Bi & Wei (2003) for both sets of scaling exponents. This is anticipated since the mixing layer is nearly homogeneous in the x and z directions, and the streamwise velocity u has more maturely developed turbulent structures. This validation of our results is encouraging and also confirms that the streamwise velocity fluctuations in sheared and unsheared turbulence have similar longitudinal and transverse relative scaling properties to homogeneous turbulence, which has been reported earlier by Ruiz-Chavarria *et al.* (2000) in a turbulent boundary layer. The transverse scaling exponents $\zeta_p^{u,z}$ are consistent among the first four sets of experiments, but are smaller than the latest simulation results of Gotoh, Fukayama & Nakano (2002). One possible explanation is relative small Reynolds numbers in the former cases, but this must be confirmed by further studies. Our results generally confirm the previous observation that transverse scaling deviates more from normal scaling than longitudinal scaling. The nature of their different degree of intermittency will be discussed later by the HS analysis.

We now analyse other sets of scaling. Figure 8 shows that the six sets of scaling exponents can be split roughly into three groups: (I) $\zeta_p^{u,x}$, $\zeta_p^{w,x}$ and $\zeta_p^{w,z}$; (II) $\zeta_p^{u,z}$ and

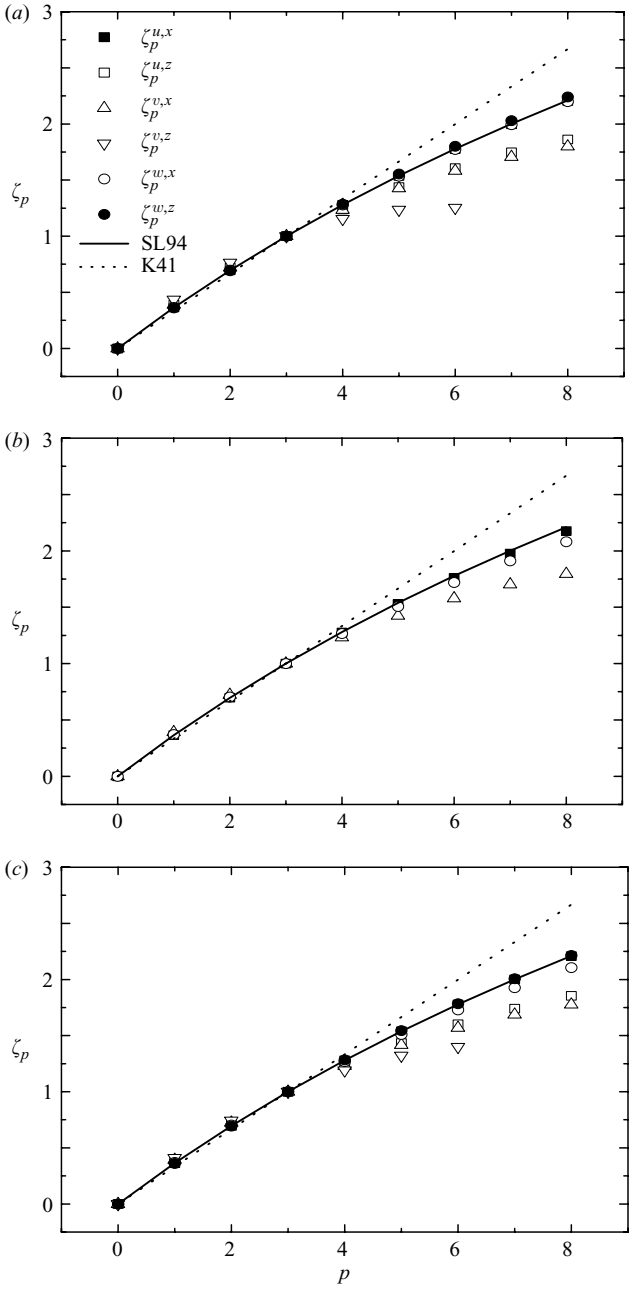

FIGURE 8. The ESS scaling exponents ζ_p for longitudinal (filled symbols) and transverse (open symbols) velocity structure functions under three flow conditions: (*a*) 40*p*, (*b*) 40*e*, (*c*) 70*e*. The highest order of the moments estimated for the transverse velocity increments v (spatial increments) goes up to 6. Note that the increments in the spanwise direction x do not have reliable scaling in the case of 40*e*, and so are omitted from the plot.

$\zeta_p^{v,x}$; (III) $\zeta_p^{v,z}$. We attempt to itemize our observations and discussions according to three groups as follows:

(*a*) The first group (I) includes two sets of longitudinal scaling ($\zeta_p^{u,x}$, $\zeta_p^{w,z}$), one obtained with the Taylor's hypothesis and the other through direct simultaneous

	Present		Bi		Chen		Shen		Gotoh	
	$R_\lambda = 237$		$R_\lambda = 500$		$R_\lambda = 216$		$R_\lambda = 254$		$R_\lambda = 381$	
Order p	$\zeta_p^{u,x}$	$\zeta_p^{u,z}$	$\zeta_p^{u,x}$	$\zeta_p^{u,z}$	$\zeta_p^{u,x}$	$\zeta_p^{u,z}$	$\zeta_p^{u,x}$	$\zeta_p^{u,y}$	$\zeta_p^{u,x}$	$\zeta_p^{u,z}$
1	0.36	0.39	0.37	0.37	0.38	0.37	0.36	0.38	0.370 ± 0.004	0.369 ± 0.004
2	0.70	0.72	0.69	0.69	0.70	0.70	0.69	0.72	0.709 ± 0.009	0.701 ± 0.01
3	1.00	1.00	1.00	1.00	1.00	1.00	1.00	1.00	1.02 ± 0.02	0.998 ± 0.02
4	1.28	1.24	1.28	1.23	1.27	1.23	1.28	1.24	1.30 ± 0.02	1.26 ± 0.03
5	1.54	1.44	1.54	1.44	1.51	1.44	1.54	1.43	1.56 ± 0.03	1.49 ± 0.04
6	1.78	1.61	1.77	1.63	1.75	1.62	1.77	1.58	1.79 ± 0.04	1.69 ± 0.05
7	2.00	1.75	1.97	1.78	1.95	1.75	1.98	1.71	1.99 ± 0.04	1.86 ± 0.05
8	2.21	1.86	2.17	1.89	2.14	1.85	2.16	1.82	2.18 ± 0.04	2.00 ± 0.04

TABLE 2. The comparison of the ESS scaling exponents obtained in the present experiment ($40p$) and several results obtained preciously by Bi & Wei (2003), Chen *et al.* (1997), Shen & Warhaft (2002), Gotoh, Fukayama & Nakano (2002), for both the longitudinal structure function ($\zeta_p^{u,x}$) and transverse structure function ($\zeta_p^{u,z}$). Data sets in the present study are extracted from figure 8.

measurement. They are very close to the results of homogeneous and isotropic turbulence given by the log-Poisson model of She & Lévêque (1994). As discussed above, both streamwise and spanwise turbulent fluctuations are close to being homogeneous. The first group also includes a transverse scaling $\zeta_p^{w,x}$ which deviates remarkably form other transverse exponents in group (II). In the present free shear flow, $\zeta_p^{w,x}$ is very close to the value predicted by SL94. Careful examination of the exponent values in table 3 shows that the three exponent values are closely equal at low orders, but $\zeta_p^{w,x}$ has slightly larger values than the other two longitudinal exponents at $p > 6$. Note that $\zeta_p^{w,x}$ is related to ω_y. On the other hand, $\zeta_p^{u,z}$ is also related to ω_y, but shows significantly smaller scaling exponents. This is a sign of strong anisotropy, and deserves further study.

(*b*) The group (II) exponents include $\zeta_p^{u,z}$ and $\zeta_p^{v,x}$ which have exponent values consistent with the transverse scaling exponents in homogeneous turbulence, which are known to have systematically smaller values than the longitudinal ones. By an extension of the argument of Chen *et al.* (1997), $\zeta_p^{u,z}$ is related to ω_y and $\zeta_p^{v,x}$ to ω_z. Then, the above result implies that the spanwise and vertical vortex structures may have a similar intermittency property. This is possible if the vortical structures on the perpendicular plane have random orientation. Note that in a mixing layer, ω_z is the primary component of vortices. A closer inspection shows that $\zeta_p^{v,x}$ is slightly more intermittent than $\zeta_p^{u,z}$, suggesting that the primary spanwise vortices are slightly more singular.

(*c*) The group (III) includes only $\zeta_p^{v,z}$ that show the largest deviation from the normal scaling and the strongest intermittency effects. By the same argument, $\zeta_p^{v,z}$ is related to streamwise vortices ω_x. Thus, the result shows that the streamwise vortices are much more intermittent than the two other vorticity components. We believe that this is plausible, and a similar situation occurs in the boundary flow with the formation of the streaks near the boundary.

Among three different flow conditions, the scaling exponents of the two longitudinal components ($\zeta_p^{u,x}$ and $\zeta_p^{w,z}$) vary little. The transverse component $\delta_x w$ has slightly more intermittent scaling when the impediment is introduced, indicating that the upstream

ζ_p\Order p	1	2	3	4	5	6	7	8
SL94	0.36	0.70	1.00	1.28	1.54	1.78	2.00	2.21
K41	0.33	0.67	1.00	1.33	1.67	2.00	2.33	2.67
40p								
$\zeta_p^{u,x}$	0.36	0.70	1.00	1.28	1.54	1.78	2.00	2.21
$\zeta_p^{u,z}$	0.39	0.72	1.00	1.24	1.44	1.61	1.75	1.86
$\zeta_p^{v,x}$	0.39	0.72	1.00	1.23	1.43	1.58	1.71	1.80
$\zeta_p^{v,z}$	0.44	0.76	1.00	1.15	1.24	1.25	–	–
$\zeta_p^{w,x}$	0.37	0.70	1.00	1.28	1.54	1.77	1.99	2.20
$\zeta_p^{w,z}$	0.36	0.69	1.00	1.29	1.55	1.80	2.03	2.24
40e								
$\zeta_p^{u,x}$	0.37	0.70	1.00	1.28	1.53	1.76	1.98	2.18
$\zeta_p^{v,x}$	0.39	0.72	1.00	1.23	1.42	1.58	1.70	1.79
$\zeta_p^{w,x}$	0.37	0.70	1.00	1.27	1.51	1.72	1.91	2.08
70e								
$\zeta_p^{u,x}$	0.36	0.70	1.00	1.28	1.54	1.78	2.00	2.21
$\zeta_p^{u,z}$	0.39	0.72	1.00	1.24	1.43	1.60	1.74	1.85
$\zeta_p^{v,x}$	0.39	0.72	1.00	1.23	1.42	1.57	1.69	1.78
$\zeta_p^{v,z}$	0.41	0.74	1.00	1.19	1.32	1.40	–	–
$\zeta_p^{w,x}$	0.37	0.70	1.00	1.27	1.51	1.73	1.93	2.11
$\zeta_p^{w,z}$	0.36	0.69	1.00	1.28	1.54	1.78	2.01	2.21

TABLE 3. The ESS scaling exponents for the two longitudinal structure functions, ($\zeta_p^{u,x}$, $\zeta_p^{w,z}$) and four transverse structure functions ($\zeta_p^{u,z}$, $\zeta_p^{v,x}$, $\zeta_p^{v,z}$, $\zeta_p^{w,x}$) under three flow conditions. Corresponding scaling exponents from K41 and SL94 models are also given for comparison.

perturbation by the impediment introduces additional intermittency to the spanwise component. Indeed, the introduction of the impediment breaks the scaling for several components at 40e, which are restored further downstream at 70e. Comparing 40p and 70e, some variation of the scaling exponents of the other transverse components may be recorded, but are not very significant. The HS analysis below is more effective in describing their difference.

In summary, we find that the two sets of longitudinal scaling are close to homogeneous scaling and to SL94 and the transverse scaling exponents are generally smaller than the longitudinal ones when $p > 3$ with the exception of $\zeta_p^{w,x}$ which are significantly less anomalous than other transverse ones. The nature of this is yet to be studied. The set of transverse scaling related to the streamwise vorticity component seems to be much more singular than any of the other components.

These findings show that in real anisotropic turbulence, the splitting into two groups of longitudinal and transverse velocity structure functions is not sufficient to describe the scaling property. The information of anisotropic flow structure is very important to the scaling property. Vice versa, both longitudinal and transverse scaling properties of all velocity components are required to provide a complete picture of anisotropic flow structures in the flow.

4.3. *β-test and γ-test*

In the previous section, we report the results of six sets of scaling, which show various degrees of deviation from the normal scaling. In this subsection, we apply the HS analysis to the data (velocity structure functions and scaling) to achieve a more synthesized description of the various components. The HS analysis consists

of the β-test and γ-test; the former verifies the existence of hierarchical similarity and measures the HS parameter β and the latter measures the degree of singularity of the most intense fluctuation structures. The objective is to construct a coherent description of the whole set of scaling in terms of two fundamental parameters related to the property of the hierarchy and of the most intense flow structures.

First, we report the results of the β-test and γ-test. The β-test consists in choosing a range of scales to calculate (2.8) using the sets of computed values of velocity structure function up to an order p_0. In the β-test, the range of scale is generally chosen to be the same as the ESS scaling range. In order to ensure the convergence, we choose to calculate the velocity structure functions $p \leqslant p_0 = 6$. The results are shown in figure 9 for all six sets of data and at all three physical conditions. It is clear that the β-test is satisfactorily passed in all cases. Once again, it is demonstrated that the hierarchical similarity is well-satisfied in turbulent fluctuations in a variety of physical conditions and for a variety of longitudinal and transverse fluctuation structures.

With one exception ($\beta^{w,z}$) (for which the determination of β is more uncertain because of a limited range of variation in hierarchical function, see figure 9*a*), the calculated HS parameter β seems to be universal in all cases, for either longitudinal or transverse velocity structure functions and either with or without impediment generating upstream spanwise variations. This is remarkable as it indicates that the parameter β is related to a global organizational property of the hierarchy and is not responsible for the different scaling observed in the free shear flow. This finding is in contrast with Boratav (1997) and Grossmann, Lohse & Reeh (1997) who claim that β must be different for longitudinal and transverse scaling (specifically $\beta^L > \beta^T$) for describing different scaling in numerical homogeneous turbulence at moderate Reynolds numbers. Our finding indicates that a larger deviation from the normal scaling does not necessarily imply a more heterogeneous hierarchy of fluctuation structures. We believe that the other parameter γ characterizing the most intense structures has more responsibility for the difference. The exact nature of the difference between the present result and two previous studies of numerical simulations (Boratav 1997; Grossmann, Lohse & Reeh 1997) is not yet known. Perhaps the β-test has to be done with caution; we have carefully chosen the range of ℓ and $p \leqslant 6$ for the calculation of β, which has been found important for obtaining a consistent estimate of β for all situations. Note that the measured β here are very close to the SL94 prediction for homogeneous isotropic turbulence: $\beta_{SL} = (2/3)^{1/3} = 0.874$.

Our finding is consistent with Camussi & Benzi (1997) and Casciola *et al.* (2001) who reported an observation of universal self-scaling $\tau_{p,q}$ of the energy dissipation fluctuations, where $\langle \epsilon_\ell^p \rangle \sim \langle \epsilon_\ell^q \rangle^{\tau_{p,q}}$. In the framework of the HS model, $\tau_{p,q}$ can be shown to depend only on β. Therefore, the universality of β implies the universality of the self-scaling of the dissipation fluctuation. We have independently calculated the GESS scaling exponents for all six velocity structure function components and for all three data sets, and have obtained consistent results (not shown here). Within 1% to 3% of statistical uncertainty, we consider that the universality of β is verified.

The universality of β may have a fundamental cause. As we discussed above, β describes the similarity between the fluctuation structures of increasing intensity, i.e. pth and $(p+1)$th HS function. Liu *et al.* (2003, 2004) have shown that a smaller β is typically associated with a field having heterogeneous compositions of a multiple nature, for which lower-intensity fluctuation structures have different properties from higher-intensity fluctuation structures. The BZ experiment at different reaction rates displays a variation of β which is associated with various phase transitions. Thus,

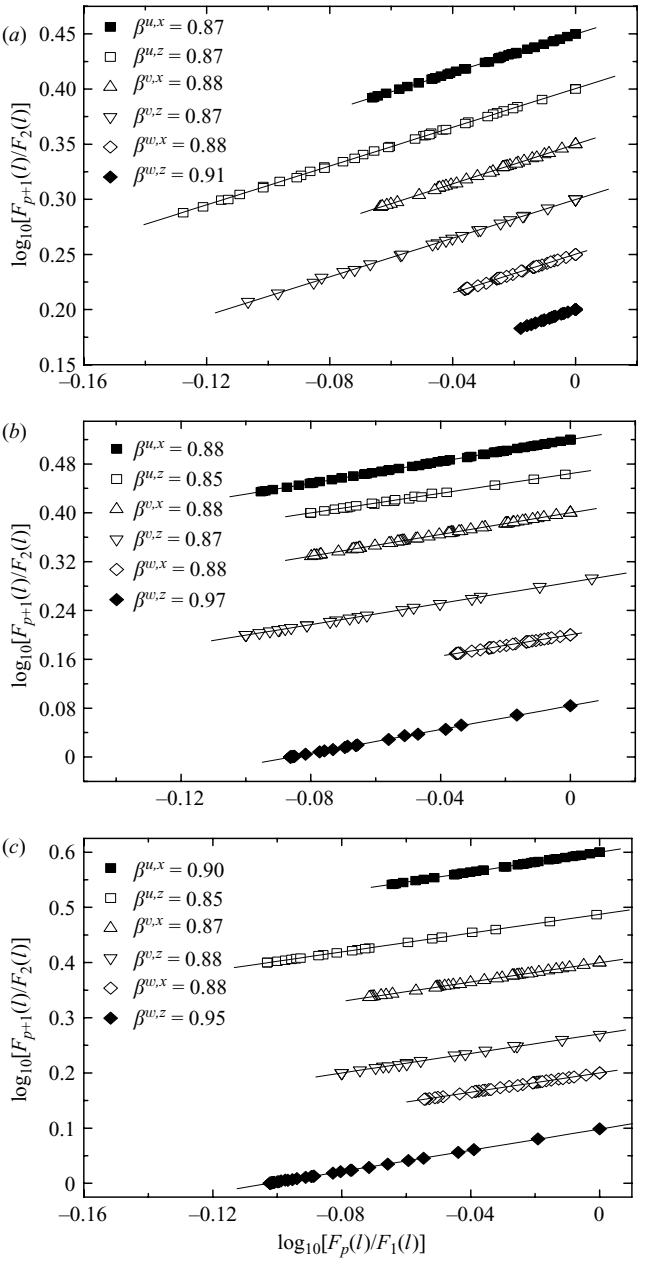

FIGURE 9. Results of the β-test of longitudinal (filled symbols) and transverse (open symbols) velocity increments of u, v and w at order $p = 6$ at three flow conditions: (*a*) 40*p*, (*b*) 40*e*, (*c*) 70*e*. For clarity, data points are shifted vertically by a suitable amount.

β is a parameter describing global organizational order of the system. In the free shear flow, although flow structures are turbulent and anisotropic, their organizational order seems to be the same for different components, and no drastic difference exists among various components. The result reported above is generally consistent with this picture. On the other hand, we observe a slight difference of β between the present free shear flow and the Couette–Taylor flow studied earlier (She *et al.* 2001). A smaller

β in the Couette–Taylor flow is, in our opinion, due to the presence of the coherent Taylor vortices that dominate the very intense fluctuations and have very distinct character from the cascade-generated low-amplitude fluctuations. In other words, the Couette–Taylor flow appears to be more heterogeneous than the free shear flow in which turbulence is generated by an upstream thread. This speculative explanation is worth testing in the future.

Note that an exceptional case is $\beta^{w,z}$ describing the longitudinal scaling of the spanwise velocity (w) along the spanwise direction (z). This quantity is obtained by analysing the difference of the two signals from simultaneous measurements by the two cross-wire probes. At present, we cannot entirely rule out the possibility of experimental errors in calculating the velocity increments of w. This is because w is a small quantity derived from two wires of the cross-wire probe and the increment is obtained by a further substraction between two probes at different z locations.

We have not attempted to quantify the errors in the β-test because our primary goal is to study the difference in scaling exponents (and hence in β) among different velocity components and among different flow conditions, for exploring mechanistic explanation in terms of flow structures. The differences are relative and the judgement of the constancy in β (and the variation below in γ) is best made on the visual inspection of the log–log plot of the β-test (see figures 9 and 10).

The γ-test consists of applying (2.10) using the value of β derived from the β-test and the measured scaling exponent ζ_p. Note that smaller γ implies a slower rate of change in high-order moments as the third-order moment varies (when the relative scaling is concerned). Since the third-order moment decreases quickly as the length scale approaches the viscous cutoff, a small γ reveals that the most intense fluctuations penetrate further into the dissipation range scales. For example, γ is zero for shocks in the Burgers equation, and the Burgers shocks have a width much smaller than a typical Kolmogorov estimate of the viscous cutoff scale. Hence, we believe this is the meaning of more singular intense structures that are characteristic of the flow environment (e.g. shocks for the Burgers equation). The γ-test focuses on the description of such characteristic structures. The HS analysis of the Couette–Taylor flow by She *et al.* (2001) shows that the variation of γ is indeed related to the breakdown of the Taylor vortex as the Reynolds number increases above 10^5.

Results of the γ-test are shown in figure 10. Here, we can classify all values of γ of various components into four groups. The first group comprises $\gamma^{u,x}$, $\gamma^{w,z}$ and $\gamma^{w,x}$ which have similarly largest values of γ or the weakest small-scale structures. With impediment (data 40*e* and 70*e*), $\gamma^{w,z}$ becomes too subtle to determine. This group corresponds to the first set of scaling with exponents close to the SL94 prediction. The values of γ (~ 0.05) are, however, a little smaller than in the longitudinal variations in homogeneous isotropic turbulence ($\gamma \sim 0.1$), indicating that the most intense associated fluctuations are a little more singular than in the isotropic situation. The fact that the transverse component $\gamma^{w,x}$ is in the same group as the other two longitudinal components is not entire understood, as we have discussed above. The second group includes $\gamma^{u,z}$ which seems to vary the most strongly with the presence of an impediment. The scaling exponents $\zeta_p^{u,z}$ of the three data sets have not shown a remarkable difference, but the β-test shows that with impediment $\beta^{u,z}$ is a little smaller, implying more heterogeneous structures in the spanwise fluctuations of u, which is very reasonable since the perturbation introduced by the impediment is in the z-direction. Note that $\gamma^{u,z}$ at 40*e* has a significantly larger values (~ 0.05) than at 40*p* (~ -0.05) and 70*e* (~ -0.01), indicating that the fluctuation structures introduced by the perturbation of the impediment seem to have a weak singularity, which later

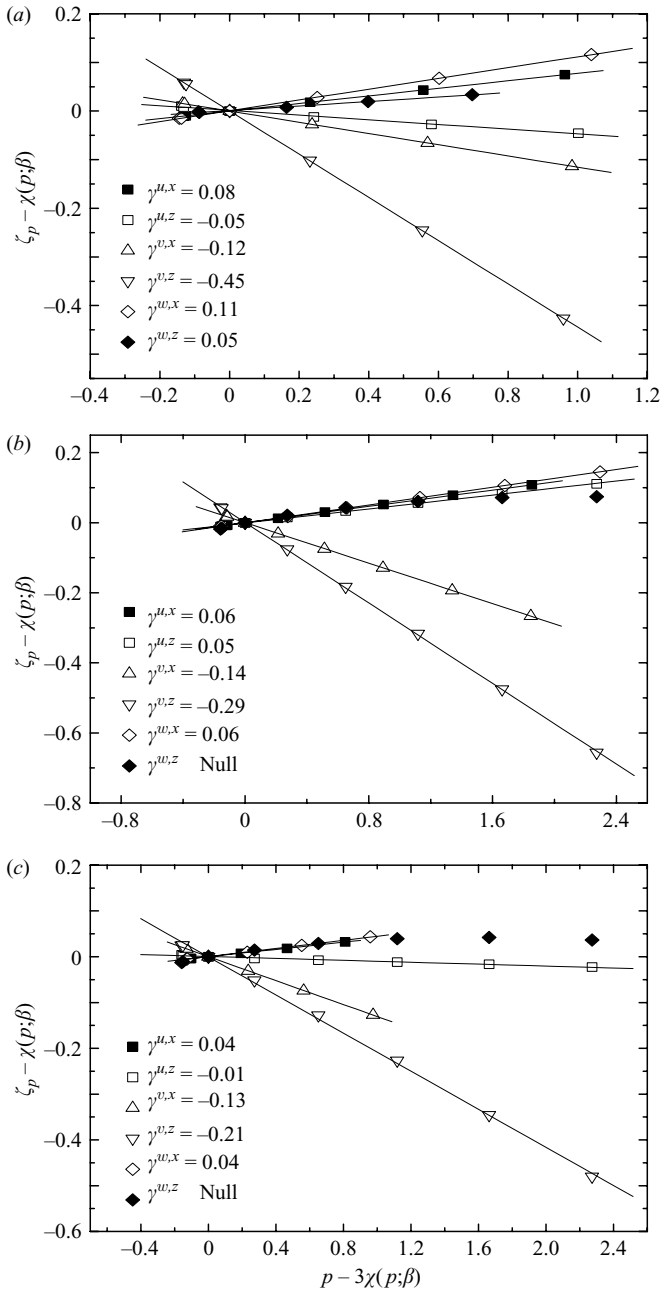

FIGURE 10. Results of the γ-test of the same data set as in figure 9.

evolves to more singular structures at 70*e*. In the present data, this component seems to carry a rich set of fluid mechanical information. The third group includes $\gamma^{v,x}$, which is another transverse component but has a less sensitive dependence on the perturbation by the impediment. The component has a very strong singularity and is related to ω_z which is the main rolling spanwise structure of a mixing layer. Our analysis seems to indicate that this component develops also very intense small-scale

Parameter	$40p$	$40e$	$70e$
$\beta^{u,x}$	0.87	0.88	0.90
$\beta^{u,z}$	0.87	0.85	0.85
$\beta^{v,x}$	0.88	0.88	0.87
$\beta^{v,z}$	0.87	0.87	0.88
$\beta^{w,x}$	0.88	0.87	0.88
$\beta^{w,z}$	0.91	0.97	0.95
$\gamma^{u,x}$	0.08	0.06	0.04
$\gamma^{u,z}$	−0.05	0.05	−0.01
$\gamma^{v,x}$	−0.16	−0.14	−0.13
$\gamma^{v,z}$	−0.45	−0.29	−0.21
$\gamma^{w,x}$	0.11	0.06	0.04
$\gamma^{w,z}$	0.05	–	–

TABLE 4. Measured HS parameter values of β and γ for all situations involving a velocity component and a direction for incremental calculation. For instance, $\beta^{u,x}$ is measured from the increment of the velocity u in the x-direction. Note that the variation of β is much smaller than γ. Thus, the HS model explains the variation of the ESS scaling through the change of the most intense fluctuation structures. See the text for detailed comments.

structures. Finally, the most singular structures is represented by $\gamma^{v,z}$ which is much smaller than all others, indicating that the associated streamwise vorticity component ($\omega_x \sim \delta_z v$) is much more singular. In other words, the streamwise vorticity is able to develop very intense fluctuation structures at very small scales, i.e. the most intense small-scale fluctuation structures are in the form of streamwise vortices. This is a distinct feature of the present free shear flow. All the values of HS parameters β and γ obtained are summarized in table 4.

Note finally that all scaling exponents in figure 8 are accurately described by the general formula (2.9) with the measured parameters β and γ. This accuracy of the HS model for all sets of scaling exponents places it as the leading choice of phenomenological models for quantitative analysis of scaling and for seeking fluid mechanical interpretation of the scaling exponents.

5. Conclusions

Free shear flow is an important system capable of generating actively evolving anisotropic turbulent structures. In this work, we have conducted a systematic study of longitudinal and transverse velocity increment statistics in a free shear flow with several kinds of upstream perturbation. The goal is to establish a relation between statistical physics concepts of scaling and fluid mechanical concepts of flow structure. A detailed investigation of the ESS scaling exponents and an analysis in the framework of the HS model reveals a possible link between flow structures and scaling. Unlike previous studies, most of which are qualitative, we focus on the quantitative understanding of the simultaneous measurements of several velocity components across multiple directions. Indeed, the free shear flows with and without the impediment provide a set of data which allows us to study the varying degree of intermittency of various small-scale anisotropic flow structures. The differentiation of flow structural properties, when linked with the calculation of scaling, begins to offer a concrete picture of how various components of flow structures organize themselves. However, the effort is just beginning and much remains to be done in applying statistical physics concepts in the description of fluid mechanical properties

of turbulence. We believe this is a step towards establishing a practical statistical fluid mechanics of turbulence, if it ever exists.

Building a statistical framework of turbulence requires a phenomenology since a direct derivation from first principles (e.g. the Navier–Stokes equation) has proved difficult, if not impossible. The HS model has been shown by previous studies and by the present work to be a sound phenomenology, since it provides an accurate description of the whole set of scaling exponents in terms of two parameters, each of which has a targeted interpretation. Since the model has been applied to the analysis of scaling properties of a wide range of nonlinear systems, the validity of the model for the free shear flow is in some sense not a surprise. However, it is a new exploration of conducting a determination of the parameter β and γ for both longitudinal and transverse increments of multiple velocity components under several flow conditions. The present study provides not only a rich set of measurement results of scaling in a free shear flow, but also offers a detailed interpretation so as to form a coherent picture of the intermittent multi-scale fluctuation field.

Let us briefly summarize our picture of small-scale structures of the free-shear-flow turbulence in light of the HS analysis. Before entering the shear layer, a boundary-layer turbulence is generated by upstream perturbations. This boundary-layer turbulence already has a small-scale component typical of boundary-layer turbulence at moderate Reynolds number, which has more intermittent small-scale structures in transverse directions than in longitudinal directions. The streamwise components have more large-scale structures than the vertical and spanwise components. After entering the mixing layer, three remarkable features are observed. First, strongly intermittent streamwise vortices are generated, which are more intermittent than in the usual transverse fluctuations of homogeneous turbulence. The strong intermittency manifests itself in very small $\gamma^{v,z}$ and also in slow decay of intense fluctuations at very small scales in spanwise increment statistics, as figure 6 shows. The component is related to streamwise vortices and the strong intermittency is observed under all three flow conditions, indicating that the mechanism is stable against upstream spanwise perturbation of the impediment. Secondly, the spanwise (z) variation of the streamwise velocity component (u) shows a remarkably sensitive dependence on the perturbation of the upstream impediment. However, the action of the impediment has led to less singular structures of u in z, namely exponent $\gamma^{u,z}$ with the impediment becomes larger and gradually decreases as the flow goes downstream. This is probably due to the generation of large-scale variations in z by the impediment, which cannot effectively generate small-scale intermittent structures in the spanwise direction. Finally, the spanwise velocity component (w) seems to generate very mild transverse fluctuations in the streamwise direction (x), which is more like a longitudinal variation than a transverse one. The exact nature of this observation is still unknown, but it seems to be also robust against the spanwise perturbation by the impediment. Other components seem to have similar behaviour to the homogeneous turbulence, so we specially outline the above three features.

It is remarkable that the HS parameter β is almost universal for fluctuations of all components under all flow conditions. This result, if confirmed for other flows, would be significant, since the universality lays a solid ground for the HS model to be a sound phenomenology for classifying turbulent flow structures. Previous studies (Liu *et al.* 2004) indicate that β changes when the system undergoes phase transitions that lead to structures of heterogeneous hierarchy. In a Newtonian fluid, this would happen if abnormal fluctuation structures are introduced to a self-organized state of fluctuations. Thus, a variation of β is a signature of new instability mechanisms or

a new turbulence production mechanism. In this regard, we would like to stress a technical point in performing the β analysis, that is, the range of ℓ must be in the scaling range and the range of p should be moderate. The results of the β-test do depend on the two ranges for which the velocity structure functions are collected.

On the other hand, we have found that the variation of γ characterizing the most intermittent structures is mostly responsible for the observed variations in the ESS scaling for various components under various flow conditions. We provide evidence that the statistical concept of the most intermittent structures within the HS phenomenology may be applicable to the description of characteristic flow structures such as streamwise vortices. A systematic relation between γ and fluid mechanical properties is still missing, but further studies on the topic would be worth pursuing.

Previous work has shown that the transverse velocity structure functions have significantly smaller scaling exponents than the longitudinal ones, i.e. $\zeta_p^T < \zeta_p^L$. Our result generally confirms this conclusion. Chen *et al.* (1997) have introduced a generalized Kolmogorov refined self-similarity hypothesis (KRSH) to relate the more intermittent transverse velocity structure functions to the locally averaged enstrophy fluctuation. We see here that various transverse components may have different degrees of intermittency when the flow anisotropy is important, hence the KRSH or the generalized KRSH may not be valid in general for all flows. Even the two transverse components of the velocity increment that are related to a single vorticity component (i.e. $\delta_x w$ and $\delta_z u$ related to ω_y) may have different scalings. We conclude that, in general, the intermittency of various components must be studied altogether for an anisotropic turbulent flow. Recent theoretical framework on SO(3) formalism may be applied in future studies (Biferale *et al.* 2002, 2004).

We thank Zhi-Xiong Zhang for drawing figure 1. We have benefited from many discussions in the LTCS of Peking University. The computation work was helped by the Turbulence Simulation Center of the LTCS. M.-D. Z. acknowledges the support by the visitor program of the Minister of Education. The work is supported by the National Natural Science Foundation of China, no. 10225210 and no. 10032020, and by the Major State Basic Project no. 2000077305.

REFERENCES

Adrian, R. J., Meinhart, C. D. & Tomkins, C. D. 2000 Vortex organization in the outer region of the turbulent boundary layer. *J. Fluid Mech.* **422**, 1–54.

Arimitsu, T. & Arimitsu, N. 2002 PDA of velocity fluctuation in turbulence by a statistics based on generalized entropy. *Physica* A **305**, 218–226.

Baroud, C., Plapp, B., Swinney, H. L. & She, Z.-S. 2003 Scaling in three-dimensional and quasi-two-dimensional rotating turbulent flows. *Phys. Fluids* **15**, 2091–2104.

Benzi, R., Ciliberto, S., Tripiccione, R., Baudet, C., Massaioli, F. & Succi, S. 1993 Extended self-similarity in turbulence flows. *Phys. Rev.* E **48**, R29–R32.

Benzi, R., Biferale, L., Ciliberto, S., Struglia, M. V. & Tripiccione, R. 1996 Scaling property of turbulence flows. *Phys. Rev.* E **53**, R3025–R3027.

Bi, W. & Wei, Q. 2003 Scaling of longitudinal and transverse structure functions in cylinder wake turbulence. *J. Turbulence* **4**, 028.

Biferale, L., Lohse, D., Mazzitelli, I. M. & Toschi, F. 2002 Probing structures in channel flow through SO(3) and SO(2) decomposition. *J. Fluid Mech.* **452**, 39–59.

Biferale, L., Calzavarini, E., Lanotte, A. S., Toschi, F. & Tripiccione, R. 2004 Universality of anisotropic turbulence. *Physica* A **338**, 194–200.

Boratav, O. N. 1997 On longitudinal and lateral moment hierarchy in turbulence. *Phys. Fluids* **9**, 3120–3122.

Boratav, O. N. & Pelz, R. B. 1997 Structures and structure functions in the inertial range of turbulence. *Phys. Fluids* **9**, 1400–1415.

Camussi, R. & Benzi, R. 1997 Hierarchy of transverse structure functions. *Phys. Fluids* **9**, 257–259.

Cantwell, B. J. 1981 Organized motion in turbulent flow. *Annu. Rev. Fluid Mech.* **13**, 437–515.

Cao, N., Chen, S. & She, Z.-S. 1996 Scalings and relative scalings in the Navier–Stokes turbulence. *Phys. Rev. Lett.* **76**, 3711–3714.

Casciola, C. M., Benzi, R., Gualtieri, P., Jacob, B. & Piva, R. 2001 Double scaling and intermittency in shear dominated flows. *Phys. Rev.* E **65**, 015301.

Casciola, C. M., Gualtieri, P., Benzi, R. & Piva, R. 2003 Scale-by-scale budget and similarity laws for shear turbulence. *J. Fluid Mech.* **476**, 105–114.

Champagne, F. H., Harris, V. G. & Corrsin, S. 1970 Experiments on nearly homogeneous turbulent shear flow. *J. Fluid Mech.* **41**, 81–139.

Chen, S., Sreenivasan, K. R., Nelkin, M. & Cao, N. 1997 Refined similarity hypothesis for transverse structure functions in fluid turbulence. *Phys. Rev. Lett.* **79**, 2253–2256.

Chen, Q., Chen, S., Eyink, G. L. & Holm, D. D. 2003 Intermittency in the joint cascade of energy and helicity. *Phys. Rev. Lett.* **90**, 214503.

Ching, E. S. C. & Kwok, C. Y. 2000 Statistics of local temperature dissipation in high Rayleigh number convection. *Phys. Rev.* E **62**, R7587–R7590.

Ching, E. S. C., Leung, C. K., Qiu, X. L. & Tong, P. 2003 Intermittency of velocity fluctuations in turbulent thermal convection. *Phys. Rev.* E **68**, 026307.

Dhruva, B., Tsuji, Y. & Sreenivasan, K. R. 1997 Transverse structure functions in high-Reynolds-number turbulence. *Phys. Rev.* E **56**, R4928–R4930.

Frisch, U. 1995 *Turbulence: The Legacy of A. N. Kolmogorov*. Cambridge University Press.

Fujisaka, H., Nakayama, Y., Watanabe, T. & Grossmann, S. 2002 Scaling hypothesis leading to generalized extended self-similarity in turbulence. *Phys. Rev.* E **65**, 046307.

Gotoh, T., Fukayama, D. & Nakano, T. 2002 Velocity field statistics in homogeneous steady turbulence obtained using a high-resolution direct numerical simulation. *Phys. Fluids* **14**, 1065–1081.

Grossmann, S., Lohse, D. & Reeh, A. 1997 Different intermittency for longitudinal and transversal turbulent fluctuations. *Phys. Fluids* **9**, 3817–3825.

Gualtieri, P., Casciola, C. M., Benzi, R., Amati, G. & Piva, R. 2002 Scaling laws and intermittency in homogeneous shear flow. *Phys. Fluids* **14**, 583–596.

Guo, H. Y., Li, L., Ouyang, Q., Liu, J. & She, Z.-S. 2003 A systematic study of spirals and spiral turbulence in a reaction-diffusion system. *J. Chem. Phys.* **118**, 5038–5044.

Jacob, B., Biferale, L., Iuso, G. & Casciola, C. M. 2004 Anisotropic fluctuations in turbulent shear flows. *Phys. Fluids* **16**(11), 4135–4142.

Kida, S. & Tanaka, M. 1994 Dynamics of vortical structures in a homogeneous shear flow. *J. Fluid Mech.* **274**, 43–68.

Kolmogorov, A. N. 1941 The local structure of turbulence in imcompressible visous fluid for very large Reynolds number. *C. R. Acad. Sci. URSS* **30**, 301–305. (Reprinted in *Proc. R. Soc. Lond.* A **434**, 9–13, 1991.

Lee, M. J., Kim, J. & Moin, P. 1990 Structure of turbulence at high shear rate. *J. Fluid Mech.* **216**, 561–583.

Lévêque, E., Ruiz-Chavarria, G., Baudet, C. & Ciliberto, S. 1999 Scaling laws for the turbulent mixing of a passive scalar in the wake of a cylinder. *Phys. Fluids.* **11**, 1869–1879.

Liu, L. & She, Z.-S. 2003 Hierarchical structure description of intermittent structures of turbulence. *Fluid Dyn. Res.* **33**, 261–286.

Liu, J., She, Z.-S., Ouyang, Q. & He, X. T. 2003 Hierarchical structures in spatially extended systems. *Intl J. Mod. Phys.* B **17**, 4139–4148.

Liu, J., She, Z.-S., Guo, H. Y., Li, L. & Ouyang, Q. 2004 Hierarchical structure description of spatiotemporal chaos. *Phys. Rev.* E **70**, 036215.

Mandelbrot, B. B. 1974 Intermittent turbulence in self-similar cascades: divergence of high moments and dimension of the carrier. *J. Fluid Mech.* **62**, 331–358.

Melander, M. V. & Hussain, F. 1993 Coupling between a coherent structure and fine-scale turbulence. *Phys. Rev.* E **48**, 2669–2689.

Mydlarski, L. & Warhaft, Z. 1996 On the onset of high-Reynolds-number grid-generated wind tunnel turbulence. *J. Fluid Mech.* **320**, 331–368.

Ouyang, Z. & She, Z.-S. 2004 Scaling and hierarchical structures in DNA Sequences. *Phys. Rev. Lett.* **93**, 078103.

Pumir, A. 1996 Turbulence in homogeneous shear flows. *Phys. Fluids* **8**, 3114–3127.

Pumir, A. & Shraiman, B. I. 1995 Persistent small scale anisotropy in homogeneous shear flows. *Phys. Rev. Lett.* **75**, 3114–3117.

Queiros-Conde, D. 1997 Geometrical extended self-similarity and intermittency in diffuson-limited aggregates. *Phys. Rev. Lett.* **78**, 4426–4429.

Robinson, S. K. 1991 Coherent motions in the turbulent boundary layer. *Annu. Rev. Fluid Mech.* **23**, 601–639.

Rogers, M. M. & Moin, P. 1987 The structure of the vorticity field in homogeneous turbulent flows. *J. Fluid Mech.* **176**, 33–66.

Ruiz-Chavarria, G., Baudet, C. & Ciliberto, S. 1994 Hierarchy of the energy dissipation moments in fully developed turbulence. *Phys. Rev. Lett.* **74**, 1986–1989.

Ruiz-Chavarria, G., Ciliberto, S., Baudet, C. & Lévêque, E. 2000 Scaling properties of the streamwise component of velocity in a turbulent boundary layer. *Physica* D **141**, 183–198.

Saddoughi, S. G. & Veeravalli, S. V. 1994 Local isotropy in trubulent boundary layers at high Reynolds number. *J. Fluid Mech.* **268**, 333–372.

She, Z.-S. 1991 Intermittency and non-Gaussian statistics in turbulence. *Fluid Dyn. Res.* **8**, 143–158.

She, Z.-S. 1998 Universal laws of cascade of turbulent fluctuations. *Prog. Theor. Phys. Suppl.* **130**, 87–102.

She, Z.-S. & Lévêque, E. 1994 Universal scaling laws in fully developed turbulence. *Phys. Rev. Lett.* **72**, 336–339.

She, Z.-S. & Liu, L. 2003 Measuring intermittency parameters of energy cascade in turbulence. *Acta Mech. Sinica* **19**, 453–457.

She, Z.-S., Aurell, E. & Frisch, U. 1992 The inviscid Burgers-equation with initial data of Brownian type. *Commun. Math. Phys.* **148**, 623–641.

She, Z.-S., Ren, K., Lewis, G. S. & Swinney, H. L. 2001 Scalings and structures in turbulent Couette–Taylor flow. *Phys. Rev.* E **64**, 016308.

She, Z.-S., Fu, Z.-T., Chen, J., Liang, S. & Liu, S.-D. 2002 Hierarchical structures in climate and atmospheric turbulence. *Prog. Nat. Sci.* **12**, 747–752.

Shen, X. & Warhaft, Z. 2002 Longitudinal and transverse structure functions in sheared and unsheared windtunnel turbulence. *Phys. Fluids* **14**, 370–381.

Sreenivasan, K. R. 1991 Fractals and multifractals in fluid turbulence. *Annu. Rev. Fluid Mech.* **23**, 539–600.

Sreenivasan, K. R. 1996 The passive scalar spectrum and the Obukhov–Corrsin constant. *Phys. Fluids* **8**, 189–196.

Sreenivasan, K. R. & Antonia, R. A. 1997 The phenomenology of small-scale turbulence. *Annu. Rev. Fluid Mech.* **29**, 435–472.

Tavoularis, S. & Corrsin, S. 1981 Experiments in nearly homogeneous turbulent shear flow with a uniform mean temperature gradient. *J. Fluid Mech.* **104**, 311–367.

Toschi, F., Amati, C., Succi, S., Benzi, R. & Piva, R. 1999 Intermittency and structure functions in channel flow turbulence. *Phys. Rev. Lett.* **82**, 5044–5047.

Toschi, F., Lévêque, E. & Ruiz-Chavarria, G. 2001 Shear effects in nonhomogeneous turbulence. *Phys. Rev. Lett.* **85**, 1436–1439.

Turiel, A., Mato, G., Parga, N. & Nadal, J.-P. 1998 Self-similarity properties of natural images resemble those of turbulence. *Phys. Rev. Lett.* **80**, 1098–1101.

Zhou, M. D., Heine, C. & Wygnanski, I. 1996 The effects of excitation on the coherent and random motion in a plane wall jet. *J. Fluid Mech.* **310**, 1–37.